Int. J. Electrochem. Sci., 9 **(2014)** 8090 - 8096

International Journal of
ELECTROCHEMICAL
SCIENCE
www.electrochemsci.org

Short Communication

Dye-sensitized Solar Cells Based on Graphene-TiO_2 Nanoparticles/TiO_2 Nanotubes Composite Films

C.B. Song, Y.H. Qiang[*]*, Y.L. Zhao, X.Q. Gu, L. Zhu， J. Song, X. Liu*

School of Materials Science and Engineering, China University of Mining and Technology, Xuzhou 221116, China
[*]E-mail: yhqiang@cumt.edu.cn

Received: 21 September 2014 / *Accepted:* 18 October 2014 / *Published:* 28 October 2014

Dye-sensitized solar cells (DSSCs) were fabricated using TiO_2 nanotube arrays (NTAs) as the photoanodes, which were adhered onto transparent conducting glass substrates by a graphene-TiO_2 composite paste. The effect of the graphene contents on the DSSC performance was investigated by adjusting the ratios of graphene to TiO_2 in the paste. It was found that the optimized DSSC efficiency of 6.29 % was achieved at a suitable loading concentration of 0.1 wt%. Furthermore, it was demonstrated that the performance enhancement was due to the promoting effect of graphene on electron transfer. However, graphene can also absorb solar light, which could lead to the decrease of light harvest of dye molecules and thus a negative effect on the power conversion efficiency of DSSCs.

Keywords: dye-sensitized solar cells; graphene; TiO_2 nanotubes; nanocomposite; electrochemical impedance spectroscopy

1. INTRODUCTION

In recent years, dye-sensitized solar cells (DSSCs) have received much attention as a potential alternative to the silicon related solar cells owing to both the high efficiency and low cost [1]. During 2012, a considerable efficiency of 12.3% has been attained in the cells with liquid electrolyte [2]. In general, the DSSC has a sandwich configuration that consists of a dye-sensitized TiO_2 photoanode, an electrolyte containing I^-/I_3^- redox couple and a Pt-coated counter electrode [3]. The TiO_2 photoanode plays an important role in loading dye and transmitting electrons. Recently, one-dimensional (1D) nanostructures such as TiO_2 NTAs have received particular attention due to a direct and fast transport passway for carriers [4-7].

To the best of our knowledge, Grime and his coworkers first reported the fabrication of a self-assembled TiO_2 NTs membrane by anodic oxidation of Ti foil in HF-containing acidic electrolyte [8].

Afterwards, by varying the fluorides and changing the aqueous electrolytes, TiO_2 NTAs of high aspect ratios and smooth surfaces were fabricated [9, 10]. Despite of those, the wider applications of TiO_2 NTAs are restricted due to both the opaque substrates and a poor electric contact between the membrane and the substrate [11]. Thus, a few attempts have been tried to obtain the full transparent photoanodes based on the TiO_2 NTAs [12-15]. Herein, in order to fix the free-standing TiO_2 NTA membranes, a conducting paste consisting of TiO_2 nanoparticles (NPs) was usually deposited onto the transparent conductive substrates as the bonding layers [16-18]. However, further improvement in DSSC efficiency is limited by the electron transferring in the TiO_2 NPs layers.

Recently, 2D graphene (G) has attracted enormous attention due to its high thermal conductivity, excellent mobility of charge carriers and extremely high theoretical specific surface area [19-21]. For example, much effort has been made on the incorporation of graphene in mesoporous TiO_2 films. Kim et al. reported that GO/TiO_2 nanocomposites can be applied as an interfacial layer between a FTO layer and a nanocrystalline TiO_2 film, and they demonstrated the enhanced conversion efficiency [22]. Yang et al. introduced graphene into the nanocrystalline anode of a DSSC, and it was shown that the conversion efficiency was increased by 39% [23]. Nevertheless, there were still few reports on the G-TiO_2 nanocomposite films as the bonding layers in TiO_2-nanotube-based DSSCs. In this study, we succeeded in preparation of G-TiO_2 bonding layers and investigated the effect of graphene contents on the total performance of DSSCs.

2. EXPERIMENTAL DETAILS

2.1 Preparation of free-standing NTAs

TiO_2 NTAs were obtained via an optimized three-step anodic oxidation process, according to our previous research paper [16]. Typically, a Ti foil was dipped into a solution of ethylene glycol containing 0.3 wt% ammonium fluoride (NH_4F) and 2 vol% H_2O while a constant voltage of 60 V was applied versus a Pt counter electrode for 1 h. Afterwards, the samples were ultrasonically washed with deionized water to remove the precipitates from the NT surface, followed by a second anodization for 3 h under the same conditions with the first anodization. Further, the obtained samples were washed ultrasonically again in the methanol and annealed at 450 $^{\circ}$C for 1 h in ambience. During the third anodization process, the duration was set up as 1 h in the same conditions of the first anodization. Finally, the samples were immersed in 10% H_2O_2 aqueous solution in order to detach the NTAs membrane from Ti substrate.

2.2 Assembly of DSSCs

Scheme 1 shows the novel structure of G-TiO_2 NPs/TiO_2 NTs bilayer photoanode. Graphene nanoplatelets, grade 3, were purchased from The Sixth Element, Inc. (China). The G-TiO_2 pastes were prepared by adding various concentrations of graphene (0.05, 0.1 and 0.15 wt%) into the pastes composed of TiO_2 NPs (size about 10 nm, Wuhan Geao). Both the pure and composite pastes were

then printed on the FTO glass substrates (15 Ω/□, Dalian Hepta Chroma) by spin-coating as bonding layers, of which the thickness were controlled by 3 M adhesive tape (Magic, USA). The trimmed TiO_2 NTAs membranes (5×5 mm^2) were transferred onto the bonding layers and then annealed at 450 ˚C for 1 h. The above prepared samples were immersed into a 3 mM ethanol solution of N719 (Dalian Hepta Chroma) for 24 h. Finally, the dye-absorbed anodes and Pt-coated counter electrodes were stacked and sealed with 60 μm thick thermal-plastic surlyn (DHS-SN1760) spacer at 110 ˚C for 15 s. An iodide-based liquid electrolyte (0.6 M DMPII, 0.03M I_2, 0.5 M TBP and 0.1 M LiI in MPN, Dalian Hepta Chroma) was injected into the devices by capillary force.

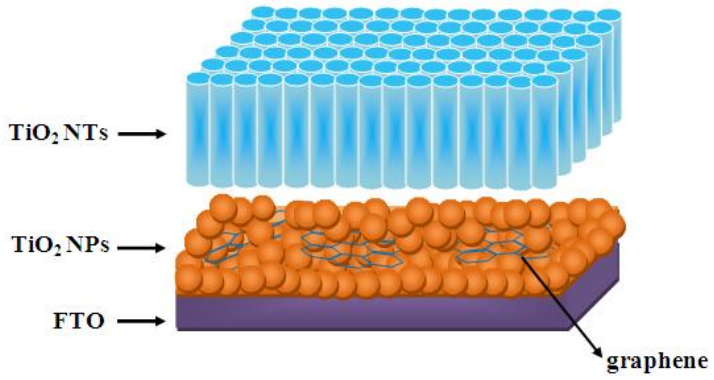

Scheme 1. Schematic illustration of the novel G-TiO_2 NPs/TiO_2 NTs bilayer photoelectrode.

2.3 Characterization and measurements

The morphology and structure were characterized by field-emission scanning electron microscopy (FESEM, S-4800) and transmission electron microscopy (TEM, Tecnai G2 F20). UV-vis absorption spectroscopy (UV-vis, Cary 300) were used to study the sunlight absorbance of the bonding layers. Photocurrent density-voltage (*J-V*) characteristics were recorded with a Keithley model 2420 digital source meter under illumination of 100 $mW \cdot cm^{-2}$ provided by a solar simulator (Beijing Trusttech). Electrochemical impedance spectroscopy (EIS) analysis was made under illumination by using an electrochemical test station (CHI660D).

3. RESULTS AND DISCUSSION

The TEM image of G-TiO_2 NPs nanocomposite is shown in Fig. 1. One can see that TiO_2 NPs with the diameters of 10-20 nm are well dispersed within the graphene, allowing good contact between graphene and TiO_2 NPs. This effect is important for introducing an alternative electrical conduction pathway into the system.

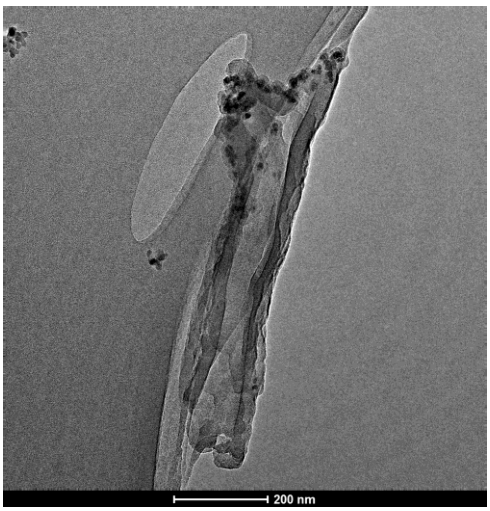

Figure 1. TEM image of TiO_2 NPs and graphene.

Fig. 2 shows the side-view FESEM image of TiO_2 NTA membrane and G-TiO_2 NPs/TiO_2 NTs electrode. It is found that the membrane is composed of many uniform, smooth, aligned and densely packed TiO_2 NTs with the diameters of ~100 nm. A clear, abrupt interface is observed between the layers, suggesting that an expected bilayer structure is obtained.

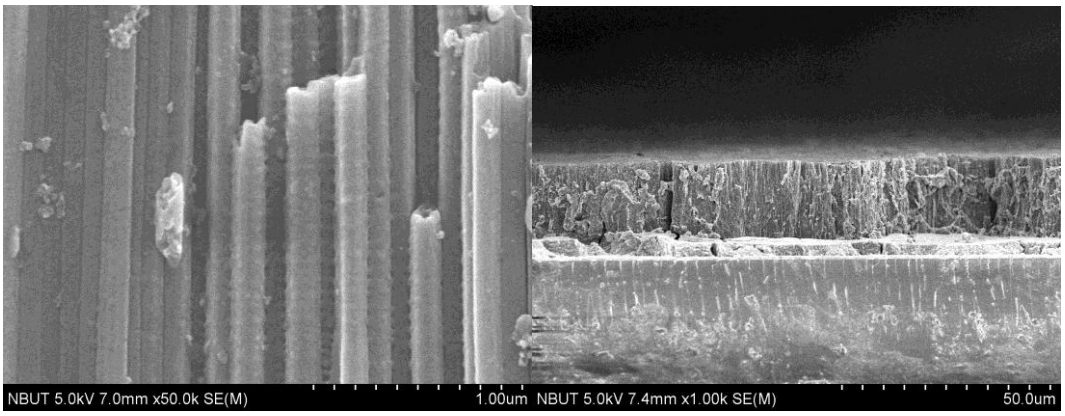

A B

Figure 2. The side-view FESEM image of TiO_2 NTA membrane and G-TiO_2 NPs/TiO_2 NTs electrode

Fig. 3 shows the EIS spectra measured at the different frequencies ranging from 10^{-2} to 10^5 Hz. Two semicircles dominate the whole curves, which correspond to charge transferring at the Pt/electrolyte and electrolyte/dye/TiO_2 interfaces, respectively [24]. Compared to those fabricated with the G-free photoanodes, the large semicircles (R_3) of DSSCs containing G/TiO_2 photoanodes are much smaller (shown in Table 1). It indicates that graphene can enhance the electron transferring. The smallest value of R_3 value is achieved at a graphene content of 0.1 wt%, which also means the fastest

electron transferring rate. However, with further increasing graphene contents (0.15 wt%), the R_3 value is increased. The behavior might be presumably attributed to the decreased light-harvesting [25].

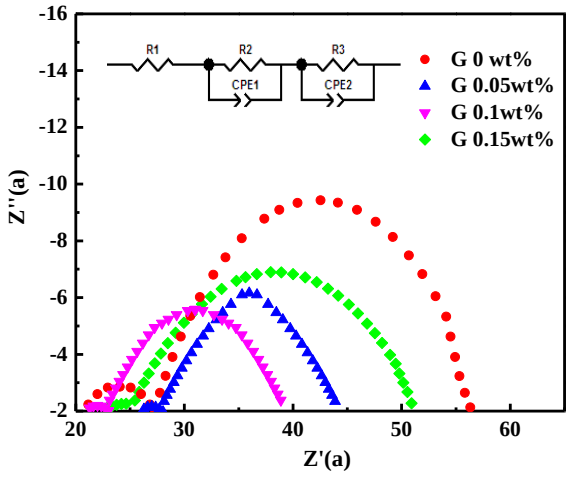

Figure 3. Nyquist plots of the DSSCs based on the G-TiO_2 NPs/TiO_2 NTs bilayer photoelectrodes. The inset indicates an equivalent circuit used for fitting the EIS results.

Fig. 4 shows the UV-vis diffuse reflectance spectra of all the bonding layers without dye-sensitized. The spectra show that the absorbance intensity of G-TiO_2 samples is higher than that of pure TiO_2 over the whole range, and the visible absorption increases with increasing the graphene loading. The increased absorbance intensity comes from graphene. Naturally, the higher the content of graphene in composites, the less the sunlight harvesting of dye molecules and thus the worse the performance of DSSCs is [26].

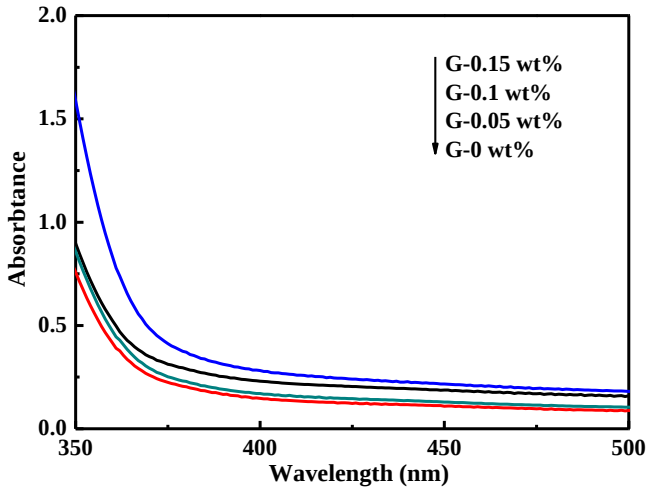

Figure 4. UV-vis absorption spectra of all the bonding layers.

Comparison of the *J-V* characteristics of the DSSCs based on G-TiO_2 NPs/TiO_2 NTs bilayer structure photoanodes with different graphene contents and pure TiO2 photoanode is shown in Fig. 5

and Table 1. As is seen, the η value of DSSCs increases from 4.35% to 6.29% with the increase in graphene content from 0 to 0.1 wt%. This is due to the fact that the incorporation of a small amount of graphene can reduce the charge recombination rate and resistance, as discussed above. Therefore, it is not surprising that the values of V_{oc} and J_{sc} of a DSSC increase in the presence of a small amount of graphene. However, at higher graphene content, the conversion efficiency decreases. A higher graphene loading causes graphene agglomeration and light-harvesting competition between the dye and graphene, and consequently increases the charge transport resistance at the electrolyte/dye/TiO_2 interface and reduces the efficiency, as stated above [27].

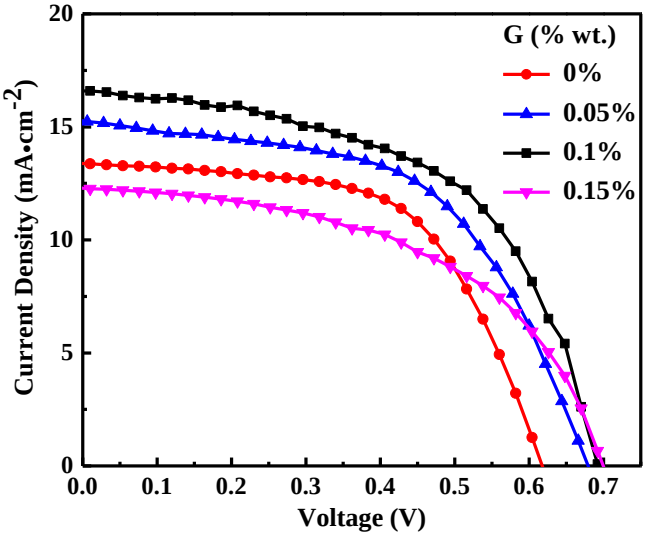

Figure 5. *J-V* curves of the DSSCs based on the G-TiO_2 NPs/TiO_2 NTs bilayer photoelectrodes with different graphene contents.

Table 1. Electron transfer resistance and photovoltaic parameters of DSSCs fabricated with G-TiO_2 NPs/TiO_2 NTs nanocomposites films.

Samples	R_3 (Ω)	J_{sc} (mA·cm^{-2})	V_{oc} (V)	FF	η (%)
0 %	33.71	12.26	0.69	0.51	4.35
0.05 %	18.27	13.26	0.69	0.61	5.67
0.1 %	14.92	16.59	0.69	0.56	6.29
0.15 %	20.44	13.36	0.63	0.57	4.87

4. CONCLUSIONS

In conclusion, DSSCs based on the novel G-TiO_2 NPs/TiO_2 NTs bilayer structure photoanodes were fabricated by a direct mechanical mixing and spin-coating method. The results showed that the incorporation of 0.1 wt% graphene into the TiO_2 pastes increased the total solar cell efficiency by 44% due to the enhanced electron transferring. However, higher graphene loading beyond the optimal concentration can cause the decrease of the efficiency due to the light shielding of graphene. This

study will provide new insight into the insight into the fabrication and structural design of highly efficient DSSCs.

ACKNOWLEDGEMENTS
This work was financially supported by the Fundamental Research Funds for the Central Universities (2013XK07) and partial supported by Natural Science Foundation of Jiangsu Province (BK20130198).

References

1. B. O'Regan, M. Grätzel, *Nature*, 353 (1991) 737
2. A. Yella, H.W. Lee, H.N. Tsao, C. Yi, A.K. Chandiran, M.K. Nazeeruddin, E.W.G. Diau, C.Y. Yeh, S.M. Zakeeruddin, M. Grätzel, *Science*, 334 (2011) 629
3. J. Sheng, L.H. Hu, S.Y. Xu, W.Q. Liu, L. Mo, H.J. Tian, S.Y. Dai, *J. Mater. Chem*., 21 (2011) 5457
4. K. Zhu, N.R. Neale, A. Miedance, A.J. Frank, *Nano Letters*, 7 (2007) 69
5. O.K. Varghese, M. Paulose, C.A. Grimes, *Nature Nanotechnology*, 4 (2009) 592
6. S.P. Albu, A. Ghicov, J.M. Macak, R. Hahn, P. Schmuki, *Nano Letters*, 7 (2007) 1286
7. C.B. Song, Y.L. Zhao, D.M. Song, L. Zhu, X.Q. Gu, Y.H. Qiang, *Int. J. Electrochem. Sci.*, 9 (2014) 3158
8. D. Gong, C.A. Grimes, O.K. Varghese, W. Hu, R.S. Singh, Z. Chen, E.C. Dickey, *J. Mater. Res.*, 16 (2001) 3331
9. J.M. Macak, H. Tsuchiya, L. Taveira, S. Aldabergerova, P. Schmuki, *Angew. Chem. Int. Edit.*, 44 (2005) 7463
10. Q.Y. Cai, M. Paulose, O.K. Varghese, C.A. Grimes, *J. Mater. Res.*, 20 (2005) 230
11. H. Park, C.D. Yang, W.Y. Choi, *J. Power Sources*, 216 (2012) 36
12. M. Paulose, H.E. Prakasam, O.K. Varghese, L. Peng, K.C. Popat, G.K. Mor, T.A. Desai, C.A. Grimes, *J. Phys. Chem. C*, 111 (2007) 14992
13. J. Wang, Z.Q. Lin, *Chem. Mater.*, 20 (2008) 1257
14. Q.W. Chen, D.S. Xu, Z.Y. Wu, Z.F. Liu, *Nanotechnology*, 19 (2008) 365708
15. C.J. Lin, Y.H. Yu, Y.H. Liou, *Appl. Catal. B-Environ.*, 93 (2009) 119
16. D. M. Song, Y.H. Qiang, Y.L. Zhao, X.Q. Gu, C.B. Song, *Appl. Surf. Sci.*, 277 (2013) 53
17. P. Roy, D.H. Kim, K.Y. Lee, E. Spiecker, P. Schmuki, *Nanoscale*, 2 (2010) 45
18. C.B. Song, Y.H. Qiang, Y.L. Zhao, X.Q. Gu, D.M. Song, L. Zhu, *Appl. Surf. Sci.*, 305 (2014) 792
19. J. Chen, K. Li, Y. Luo, X. Guo, D. Li, M. Deng, *Carbon*, 47 (2009) 2704
20. M.J. Allen, V.C. Tung, R.B. Kaner, *Chem. Rev.*, 110 (2010) 132
21. Q.J.Xiang, J.G. Yu, *Nanoscale*, 3 (2011) 3670
22. S.R. Kim, M.K. Parvez, M. Jaroniec, *Chem. Phys. Lett.*, 483 (2009) 124
23. N. Yang, J. Zhai, D. Wang, Y. Chen, L. Jiang, *ACS Nano*, 4 (2010) 887
24. T.W. Hamann, R.A. Jensen, A.B.F. Martinson, H.V. Ryswyk, J.T. Hupp, *Energy Environ. Sci.*, 1 (2008) 66
25. I. Mora-Sero, S. Gimenez, F. Fabregat-Santiago, R. Gomez, Q. Shen, T. Toyoda, J. Bisquert, *Accounts Chem. Res.*, 42 (2009) 1848
26. H. Wang, S.L. Leonard, Y.H. Hu, *Ind. Eng. Chem. Res.*, 52 (2012) 10613
27. T. Chen, W.H. Hu, J.L. Song, G.H. Guai, C.M. Li, *Adv. Funct. Mater.*, 22 (2012) 5245

© 2014 The Authors. Published by ESG (www.electrochemsci.org). This article is an open access article distributed under the terms and conditions of the Creative Commons Attribution license (http://creativecommons.org/licenses/by/4.0/).